ANALYTICAL SCIENCES JUNE 2017, VOL. 33

Notes

Nanostructures Integrated with a Nanochannel for Slowing Down DNA Translocation Velocity for Nanopore Sequencing

Xiaoyin SUN,[*1,*2†] **Takao YASUI,**[*1,*2,*3] **Takeshi YANAGIDA,**[*4,*5] **Noritada KAJI,**[*1,*2,*3] **Sakon RAHONG,**[*1,*2] **Masaki KANAI,**[*4] **Kazuki NAGASHIMA,**[*4] **Tomoji KAWAI,**[*5] **and Yoshinobu BABA**[*1,*2,*6]

*1 *Department of Applied Chemistry, Graduate School of Engineering, Nagoya University, Furo-cho, Chikusa, Nagoya 464–8603, Japan*
*2 *ImPACT Research Center for Advanced Nanobiodevices, Nagoya University, Furo-cho, Chikusa, Nagoya 464–8603, Japan*
*3 *PRESTO, Japan Science and Technology Agency (JST), 4-1-8 Honcho, Kawaguchi, Saitama 332–0012, Japan*
*4 *Institute of Materials Chemistry and Engineering, Kyushu University, 6-1 Kasuga-Koen, Kasuga, Fukuoka 816–8580, Japan*
*5 *Institute of Scientific and Industrial Research, Osaka University, 8-1 Mihogaoka-cho, Ibaraki, Osaka 567-0047, Japan*
*6 *Health Research Institute, National Institute of Advanced Industrial Science and Technology (AIST), Takamatsu 761-0395, Japan*

Here, we developed a device integrated with a nanochannel and nanostructures to slow DNA translocation velocity. We found that translocation velocity of a single DNA molecule inside a nanochannel was decreased by pre-elongating it using some nanostructures, such as a shallow channel or nanopillars. This decrease of the translocation velocity was associated with the DNA mobility change, which is an intrinsic parameter of DNA molecules and unaffected by an electric field.

Keywords DNA mobility, single DNA molecule, nanochannel, shallow channel, nanopillars

(Received December 22, 2016; Accepted January 24, 2017; Published June 10, 2017)

Introduction

Nanopore DNA sequencing has the potential to sequence single DNA molecules with some advantages, such as higher accuracy, longer read length, higher throughput, and lower cost.[1] However, the biggest problem with nanopore DNA sequencing is that single DNA molecules translocate through the nanopore too fast to identify individual DNA bases because an electric field is concentrated around the nanopore.[2] Therefore, slowing down DNA velocity through the nanopore is crucial for developing highly sensitive nanopore DNA sequencing technology. Recently, nanostructures have been integrated with micro-nanodevices to achieve faster nanopore DNA sequencing.[3,4] In this work, we attempted to slow down DNA velocity in a nanochannel, which is a simulant structure of a nanopore, by combining nanometer-scale shallow channel and nanopillar array. Because these nanostructures can increase the electric resistance in the area and thus the electric field in the nanochannel located in close vicinity is decreased, we expected to slow down DNA in the nanochannel. In addition, the nanostructures can elongate single DNA molecules before the introduction into the nanochannel and further decrease of DNA velocity was expected due to the friction force in the nanochannel Therefore, we measured DNA velocity and calculated mobility inside nanochannels that were 300-nm wide and 300-nm tall. Additionally, the mobility of a single DNA molecule was slowed down by using a device in which nanostructures were integrated with nanochannels.

† To whom correspondence should be addressed.
E-mail: sun.xiaoyin@h.mbox.nagoya-u.ac.jp

Experimental

Device dimensions

Three types of devices were fabricated on quartz substrates, and their schematic illustrations are shown in Fig. 1. Nanochannels inside the three types of devices were designed with dimensions of 300 nm × 300 nm × 250 μm (width × height × length). For the type 1 device (Figs. 1a and 1b), two microchannels was connected with a nancochannel. The microchannels were 2-μm tall and 5-mm long, and their width was designed as a trapezium with a topline of 8.25 μm and baseline of 7 mm. The type 2 device (Figs. 1c and 1d) was designed based on the type 1 device, and a shallow channel with dimensions of 30 μm × 300 nm × 70 μm (width × height × length) was fabricated in front of the nanochannel only at one side of the microchannel. The type 3 device (Figs. 1e and 1f) was designed based on the type 2 device, and nanopillars that were 300-nm tall, 500 nm in diameter, and 1 μm in space were fabricated on a shallow channel. The fabrication process for the nanochannel devices has previously been described in detail.[5]

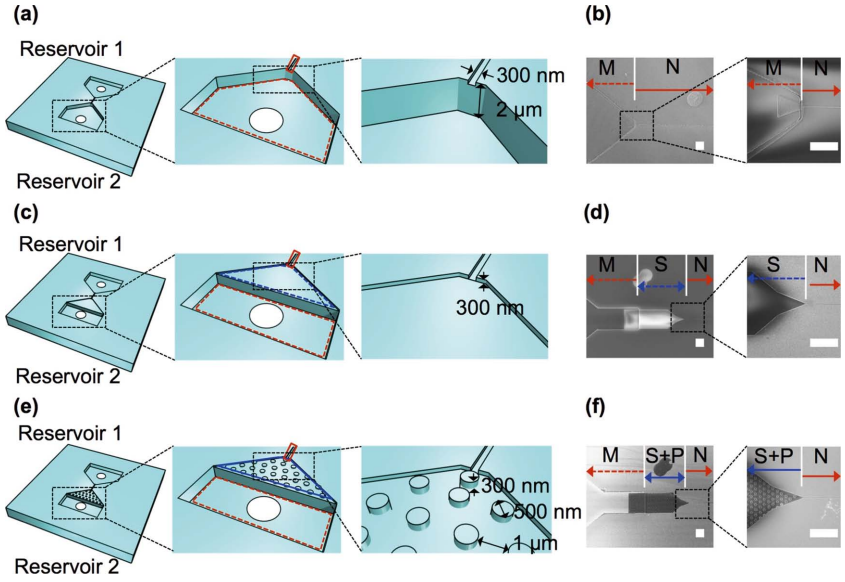

Fig. 1 Schematic and scanning electron microscope images of the nanochannel devices. (a, b) Type 1 device. (c, d) Type 2 device. (e, f) Type 3 device. Scale bars are 10 μm. Red dashed and solid lines show the microchannel and the nanochannel, respectively. A blue dashed line in (c) and a blue solid line in (e) show the shallow channel and shallow channel with nanopillars, respectively. M, N, S and S + P in (b, d, f) correspond to microchannel, nanochannel, shallow channel and shallow channel with nanopillars, respectively.

DNA sample preparation

T4 DNA molecules (166 kbp, T4GT7 DNA, Nippon Gene Co., Ltd.) and 7 kbp DNA (Thermo Fisher Scientific Inc.) were used and stained with YOYO-1 at a molar ratio of 1:5 to the total number of base pairs in each sample. For single DNA molecule observations using a microscope, DNA samples were diluted to 5 ng mL^{-1} with TE buffer (TE (pH 8.0), Nippon Gene Co., Ltd.) and stored in a freezer before use.

Experimental procedure

DNA sample and 5X TBE buffer were injected into reservoir 1 and 2, respectively (Fig. 2a). Under an applied voltage of 3 V (Model 236, Keithley) between the two reservoirs (Fig. 2a), negatively charged DNA molecules were introduced into a nanochannel *via* one side of the microchannel. Fluorescence images (Fig. 2b) of DNA translocation inside a nanochannel were obtained with an inverted fluorescent microscope (ECLIPSE TE300, Nikon) coupled with a CCD camera (C7190-43, Hamamatsu Photonics K.K.) through a 100×/1.40 NA objective lens. A 488-nm laser (FLS-448-20, Sigma Koki Co., Ltd.) was used as a light source to observe the fluorescently stained DNA. Additionally, the fluorescence images were recorded on a DV tape (Sony DV 180 ME Digital Video Cassette, Sony Corp.). Then, DNA translocation distance and time inside a nanochannel were analyzed using image-processing software (Cosmos 32, Library). Then, DNA translocation velocity was calculated using the DNA translocation distance and time. Finally, DNA mobility was calculated using $\mu = v/E_{\text{nanochannel}}$, where μ is DNA mobility, v is DNA translocation velocity, and $E_{\text{nanochannel}}$ is the electric field of the nanochannel.

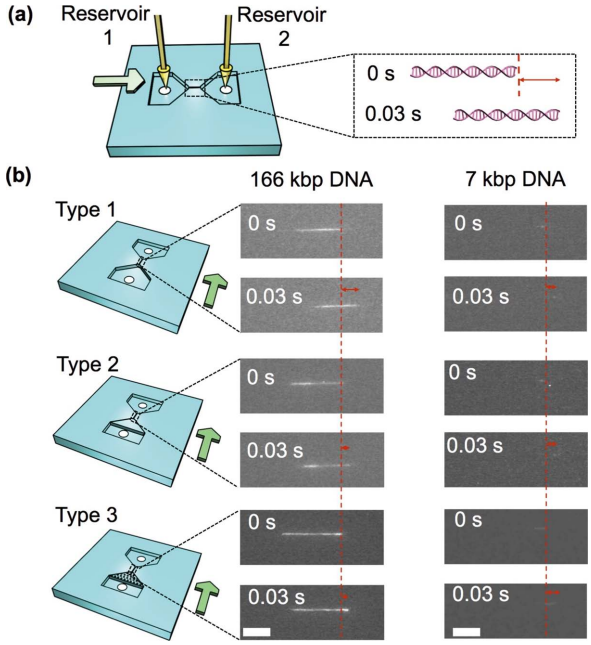

Fig. 2 (a) A schematic illustration showing the measurement procedure for DNA translocation velocity inside a nanochannel. Red dashed line shows the position of DNA head at 0 s. Red arrow shows DNA translocation distance in 0.03 s. (b) Fluorescence trajectories of 166 and 7 kbp DNA inside a nanochannel in the type 1, 2, and 3 devices. Scale bars are 10 μm. Green arrows show direction of DNA electrophoretic migration.

Results and Discussion

In the case of type 1 device, DNA molecules were introduced into the nanochannel from one side of the microchannel by applying 3 V across the reservoir 1 and 2 (Fig. 2a). DNA translocation velocity was obtained by measuring the migration distance of DNA head, L, in 0.03 s inside a nanochannel. DNA mobility was calculated by using $\mu = v/E_{\text{nanochannel}}$, where μ is

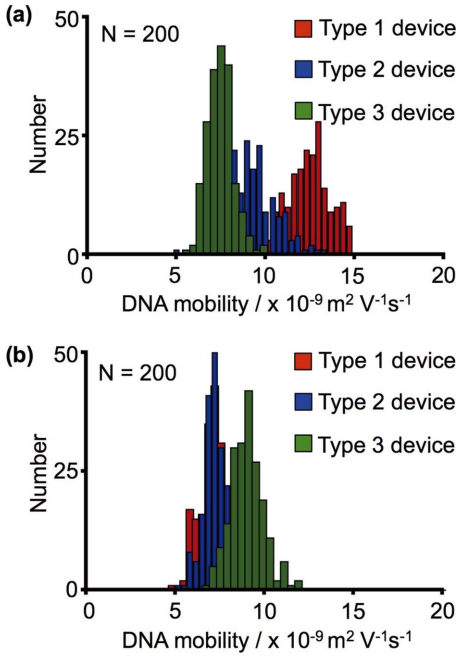

Fig. 3 DNA mobility histograms for the type 1, 2, and 3 devices. (a) 166 kbp DNA. (b) 7 kbp DNA.

DNA mobility, v is DNA translocation velocity, and $E_{\text{nanochannel}}$ is the electric field of the nanochannel. In case of type 2 and 3 devices, DNA molecules were introduced into the nanochannel from a microchannel on the side of reservoir 1, which has a shallow channel or shallow channel with nanopillars, and the translocation velocity was measured. Fluorescence images of 166 kbp DNA and 7 kbp DNA inside the nanochannels are shown in Fig. 2b.

DNA translocation velocity was measured inside a nanochannel while translocating through the type 1, 2, and 3 devices (Fig. 3). We found that the calculated mobility of 166 kbp DNA was different when translocating through a nanochannel in the type 1, 2, and 3 devices (Fig. 3a). However, 7 kbp DNA translocated through a nanochannel with a uniform mobility for the type 1 and 2 devices (Fig. 3b). Surprisingly, the mobility of 7 kbp DNA increased when translocating through a nanochannel in the type 3 device compared with the type 1 and 2 devices.

The most important factor affecting DNA translocation velocity is the variation of electric fields in the nanochannels. An electric field of a nanochannel can be decreased by increasing the resistance of the nanostructure located immediately inside of the nanochannel. Resistances inside the nanochannels are calculated in Tables S1, S2, and S3 (Supporting Information). The variation of DNA mobility in our work could not be explained by the different electric fields because DNA mobility is not substantially influenced by an electric field. The variation of friction force against DNA molecules inside the nanochannels might be considered to explain our results because DNA mobility can be evaluated as;

$$\mu = \frac{q}{f} \tag{1}$$

where q is the effective charge of the DNA and f is the electrophoretic friction coefficient when DNA translocates inside a nanochannel.[6] The electrophoretic friction is the force exerted by hydrodynamic resistance and surface friction when DNA translocate inside a nanochannel. The electrophoretic friction coefficient of DNA inside a nanochannel is directly proportional to DNA length.[7] Therefore, this equation indicates that the mobility of DNA with the same effective charge can be decreased by increasing the DNA electrophoretic friction coefficient by increasing the DNA length inside the nanochannel.

To estimate the length change of DNA inside a nanochannel, we compared the gyration radii of 166 kbp DNA and 7 kbp DNA to the dimensions of the type 1, 2, and 3 devices. In a theoretical model, DNA has a spherical shape in free solution, and the gyration radius can be evaluated using the Kratky–Porod model:[8]

$$R_{\text{g}} = \frac{1}{\sqrt{6}}\sqrt{0.68 N l_{\text{p}}} \tag{2}$$

where R_{g} is the gyration radius of DNA, N is the total number of monomers, and l_{p} is the persistence length of double-strand DNA. Based on the above equation, the gyration radii of 166 kbp DNA and 7 kbp DNA were calculated as 970 and 199 nm, respectively. DNA can be elongated by introducing some spaces with a dimension less than twice the gyration radius of DNA.[9] The space can be defined as a nanochannel in the type 1 device, the shallow channel and nanochannel in the type 2 device, and a nanopillar area and nanochannel in the type 3 device.

We found that 166 kbp DNA elongated inside a nanochannel when translocating through the type 1, 2, and 3 devices. With the type 1 device, 166 kbp DNA formed a 3D sphere inside the microchannel, and any part of 166 kbp DNA that was close enough to the nanochannel entrance was preferably introduced into the nanochannel. Additionally, this behavior resulted in a relatively short length for 166 kbp DNA inside the nanochannel.[10] With the type 2 device, 166 kbp DNA was confined and pre-elongated inside the shallow channel before being introduced into the nanochannel because the gyration radius of 166 kbp DNA is larger than the height of the shallow channel. Moreover, the pre-elongation of 166 kbp DNA resulted in a longer length inside the nanochannel. With the type 3 device, 166 kbp DNA was additionally confined and pre-elongated inside the nanopillar area before being introduced into the nanochannel because the gyration radius of 166 kbp DNA is larger than the height and width of the nanopillar area. The additional pre-elongation of 166 kbp DNA gave it the longest length inside the nanochannel. Length of 166 kbp DNA inside the nanochannels of type 1, 2 and 3 devices was measured as shown in Fig. S1 (Supporting Information). Nevertheless, there was no length change for 7 kbp DNA inside the nanochannel even when translocating through the type 1 and 2 devices because its gyration radius is smaller than the height of the shallow channel. However, 7 kbp DNA had a shorter length inside the nanochannel when translocating through the type 3 device. Because the gyration radius of 7 kbp DNA is smaller than the height and width of a nanopillar, it collided with the nanopillars and retained a coil conformation inside the nanopillar area. Additionally, 7 kbp with a coil conformation was immediately introduced into the nanochannel, thus resulting in a shorter length inside the nanochannel when translocating through the type 3 device. In order to confirm the strategy, 166 kbp DNA was introduced into the nanochannels of type 2 and 3 devices from the another microchannel on the side of reservoir 2, which does not have a shallow channel or shallow channel with nanopillars. Although it has a wide deviation, the mobilities of 166 kbp DNA inside the nanochannels did not show a significant difference between these three devices. (Fig. S2, Supporting Information).

In summary, we slowed the translocation velocity of a single DNA molecule by using a device in which nanostructures were integrated with a nanochannel. We conclude that the mobility change of DNA was due to a change in DNA length inside the nanochannel because DNA was confined and elongated by the shallow channel and nanopillar area before being introduced into the nanochannel. We propose that our device has great potential for biotechnology applications, such as nanopore DNA sequencing and single DNA manipulation and analysis.

Acknowledgements

This research was supported by the Cabinet Office, Government of Japan, and the Japan Society for the Promotion of Science (JSPS) through the Funding Program for World-Leading Innovative R&D on Science and Technology (FIRST Program), the ImPACT Program of the Council for Science, Technology, and Innovation (Cabinet Office, Government of Japan), the Nanotechnology Platform Program (Molecule and Material Synthesis) of the Ministry of Education, Culture, Sports, Science, and Technology (MEXT), Japan, a JSPS Grant-in-Aid for Scientific Research (A) 24241050, and a Grant-in-Aid for Scientific Research on Innovative Areas “Molecular Science” No. 26107709 from the MEXT and PRESTO, Japan Science and Technology Agency (JST).

Supporting Information

This material is available free of charge on the Web at http://www.jsac.or.ip/analsci/.

References

1. Y. Wang, Q. Yang, and Z. Wang, *Front. Genet.*, **2013**, *5*, 449.
2. B. M. Venkatesan and R. Bashir, *Nat. Nanotech.*, **2011**, *6*, 615.
3. S. Rahong, T. Yasui, T. Yanagida, K. Nagashima, M. Kanai, G. Meng, Y. He, F. Zhuge, N. Kaji, T. Kawai, and Y. Baba, *Anal. Sci.*, **2015**, *31*, 153.
4. N. Kaji and Y. Baba, *Anal. Sci.*, **2014**, *30*, 859.
5. X. Sun, T. Yasui, T. Yanagida, N. Kaji, S. Rahong, M. Kanai, K. Nagashima, T. Kawai, and Y. Baba, *Sci. Technol. Adv. Mater.*, **2016**, *17*, 1.
6. O. Tu, T. Knott, M. Marsh, K. Bechtol, D. Harris, D. Barker, and J. Bashkin, *Nucleic Acids Res.*, **1998**, *26*, 2797.
7. C. Reccius, J. Mannion, J. Cross, and H. Craighead, *Phys. Rev. Lett.*, **2005**, *95*, 268101.
8. J.-L. Viovy, *Rev. Mod. Phys.*, **2000**, *72*, 813.
9. G. B. Salieb-Beugelaar, K. D. Dorfman, A. van den Berg, and J. C. T. Eijkel, *Lab Chip*, **2009**, *9*, 2508.
10. J. T. Mannion, C. H. Reccius, J. D. Cross, and H. G. Craighead, *Biophys J.*, **2006**, *90*, 4538.